

The Ionization of the Local Interstellar Medium, as Revealed by FUSE Observations of N, O and Ar toward White Dwarf Stars¹

E. B. Jenkins², W. R. Oegerle³, C. Gry^{4,5}, J. Vallerga⁶, K. R. Sembach³, R. L. Shelton³, R. Ferlet⁷, A. Vidal-Madjar⁷, D. G. York⁸, J. L. Linsky⁹, K. C. Roth³, A. K. Dupree¹⁰ and J. Edelstein⁶

ABSTRACT

FUSE spectra of the white dwarf stars G191-B2B, GD 394, WD 2211 – 495 and WD 2331 – 475 cover the absorption features out of the ground electronic states of N I, N II, N III, O I and Ar I in the far ultraviolet, providing new insights on the origin of the partial ionization of the Local Interstellar Medium (LISM), and for the case of G191-B2B, the interstellar cloud that immediately surrounds the solar system. Toward these targets the interstellar abundances of Ar I, and sometimes N I, are significantly below their cosmic abundances relative to H I. In the diffuse interstellar medium, these elements are not likely to be depleted onto dust grains. Generally, we expect that Ar should be more strongly ionized than H (and also O and N whose ionizations are coupled to that of H via charge exchange reactions) because the cross section for the photoionization of Ar I is very high. Our finding that Ar I/H I is low may help to explain the

¹Based on data obtained for the Guaranteed Time Team by the NASA-CNES-CSA FUSE mission operated by the Johns Hopkins University. Financial support to U.S. participants has been provided by NASA contract NAS5-32985.

²Princeton University Observatory, Princeton, NJ 08544-1001

³Dept. of Physics and Astronomy, Johns Hopkins University, 3400 N. Charles St. Baltimore, MD 21218-2686

⁴ISO Data Center, ESA Astrophysics Division, PO Box 50727, 28080 Madrid, Spain

⁵Laboratoire d'Astronomie Spatiale, B.P.8, 13376 Marseille cedex 12, France

⁶Space Sciences Laboratory, University of California, Berkeley, CA 94720-7450

⁷Institut d'Astrophysique de Paris, 92 bis, Blvd. Arago, Paris 7504, France

⁸Dept. of Astronomy and Astrophysics, University of Chicago, 5640 Ellis Ave., Chicago, IL 60637

⁹JILA, Univ. of Colorado and NIST, Boulder, CO 80309-0440

¹⁰Smithsonian Astrophysical Observatory, 60 Garden St., Cambridge, MA 02138

surprisingly high ionization of He in the LISM found by other investigators. Our result favors the interpretation that the ionization of the local medium is maintained by a strong EUV flux from nearby stars and hot gases, rather than an incomplete recovery from a past, more highly ionized condition.

Subject headings: ISM: abundances — ISM: clouds — stars: white dwarfs — ultraviolet: ISM

1. Introduction

Our solar system is traveling through a low-density ($n_H \sim 0.1 - 0.3 \text{ cm}^{-3}$), warm ($T \approx 7000\text{K}$), partially ionized gas cloud called the Local Interstellar Cloud (LIC) (Lallement et al. 1996) with a diameter of about 4 pc (Redfield & Linsky 2000). Near the LIC are similar clouds that give rise to absorption features with different velocities (Gry 1996; Lallement 1996), known collectively as the Local Interstellar Medium (LISM). From the available evidence, the physical conditions in the LISM clouds are only slightly different from those of the LIC (Linsky 1996; Ferlet 1999).

Presently, we do not have a clear understanding of the physical processes that are responsible for high fractional ionization of helium in the LISM. From observations that $\langle n(\text{He I})/n(\text{H I}) \rangle = 0.07$ (Dupuis et al. 1995), along with the knowledge that $\text{He}/\text{H} = 0.10$ in all forms, it is evident that He is usually slightly more ionized than H. Also, helium shows less variability in how strongly it is ionized from one region to the next (Wolff, Koester, & Lallement 1999). While the EUV radiation from white dwarf and other stars can explain the observed fractional ionization of H (Vallerga 1998), these sources do not produce enough photons with energies above 24.6 eV to explain the ionization of He. To resolve this problem, two main proposals have been offered. One is that the LISM is not in a steady-state condition; it is returning from a much more highly ionized state produced by an energetic event in the recent past ($t \lesssim 10^6 \text{ yr}$), such as the flash from a nearby supernova (Reynolds 1986; Frisch & Slavin 1996) or its shock wave (Lyu & Bruhweiler 1996). The other possibility is that the ionization of He is maintained in a steady state by the diffuse EUV radiation arising from conductive interfaces between the cloud edges and the surrounding, hot medium at $T \sim 10^6 \text{ K}$ (Slavin 1989; Slavin & Frisch 1998), or, alternatively, by recombination radiation from highly ionized but cooled gases that might surround us (Breitschwerdt & Schmutzler 1994).

Sofia & Jenkins (1998) have proposed that the apparent abundances of the neutral forms of N, O and Ar, elements that are generally very lightly depleted in the interstellar

medium (if at all), can help to unravel the mystery of the He ionization. UV absorption lines in the spectra of white dwarf stars present good opportunities for studying these abundances in the LISM, since most of the brighter objects are well removed from major gas clouds elsewhere and remain immersed within a “Local Bubble” (diam. ~ 200 pc) of very hot, low density material surrounding the nearby cloud complex (Cox & Reynolds 1987; Sfeir et al. 1999). We report here on initial spectra of four white dwarf stars taken with the Far Ultraviolet Spectroscopic Explorer (FUSE) (Moos et al. 2000; Sahnou et al. 2000) taken at a resolution of $20 - 25 \text{ km s}^{-1}$ (§§2–3), and we interpret the findings in the light of the Sofia & Jenkins proposal to obtain a better understanding on how the LISM is ionized (§4).

2. Observations

The stars, their locations in the sky, estimates for $N(\text{H I})$ arising from the LIC only, and the wavelength ranges observed by FUSE are summarized in Table 1. All of the stars are at distances that range between approximately 50–80 pc. The values of $N(\text{H I})_{\text{LIC}}/N(\text{H I})$ (cf. Tables 1 and 3) indicate that the line of sight to G191-B2B contains mostly material from the LIC, while those toward the remaining three stars are dominated by other clouds in the LISM.

Our spectra cover the important absorption features from N, O and Ar in their neutral forms. In addition, for some stars we recorded two ionized forms of nitrogen, N II and N III. While the N III feature conceivably might arise from photospheric absorption, we see no evidence of stronger absorption from N III in an excited fine-structure level – in the absence of saturation this feature would be twice as strong as the one we observed if all of the N III absorption came from the star’s photosphere. Two spectral segments for one of the stars, WD 2211 – 495, are shown in Fig. 1.

Table 1. Target Stars, Locations and Wavelengths Ranges

Star ^a	ℓ (deg)	b (deg)	$\log N(\text{H I})$ for the LIC ^b	λ Coverage (Å)
G191-B2B	156.0	+7.1	18.25	987 – 1082
GD 394	91.4	1.1	17.68	987 – 1082
WD 2211 – 495	345.8	–52.6	16.73	905 – 1082
WD 2331 – 475	334.9	–64.8	17.12	905 – 1082

^aOrdered according to increasing foreground $N(\text{H I})$ – see Table 3

^bEstimate for the contribution to the hydrogen column that arises from the Local Interstellar Cloud surrounding our solar system, according to Redfield & Linsky (2000).

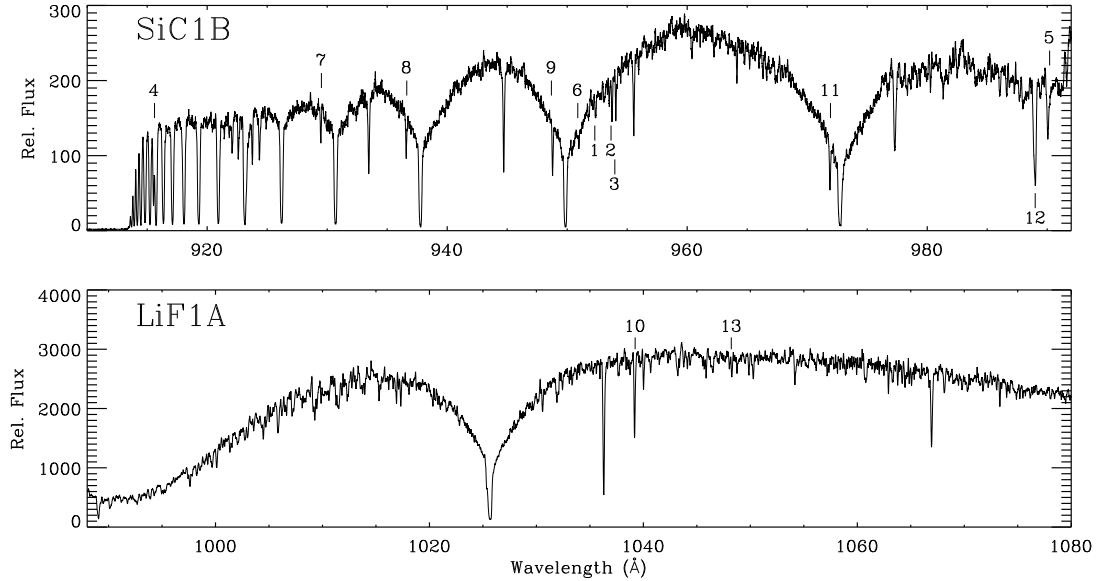


Fig. 1.— Far ultraviolet spectra of WD 2211–495 recorded by FUSE. Important features for our study are identified according to the numbers listed in the last column of Table 2.

Table 2. FUSE Measurements of Absorption Lines

Species	λ (Å)	$\log(f\lambda)^a$	WD 2211 – 495 [$W_\lambda(\text{mÅ})$]	WD 2331 – 475 [$W_\lambda(\text{mÅ})$]	Ident. in Fig. 1
N I ...	952.303	0.532 ^b	16.9 ± 2.4	...	1
	965.041	0.589	...	14.6 ± 4.2	...
	954.104	0.809	4.8 ± 1.5
	964.626	0.959	...	23.4 ± 4.1	...
	953.415	1.098	...	34.6 ± 4.5	...
	963.990	1.154	...	22.4 ± 4.2	...
	953.655	1.376	24.5 ± 2.1	34.4 ± 4.1	2
	953.970	1.521	23.2 ± 2.0	47.4 ± 4.8	3
N II ...	915.612	2.180	$89. \pm 15.^c$	$59. \pm 20.^c$	4
N II* ..	916.012	2.180 ^b	-2.7 ± 2.9^d	-2.9 ± 5.3^d	...
N II** .	916.701	2.182 ^b	3.6 ± 2.8^d	-9.0 ± 5.7^d	...
N III ..	989.799 ^e	2.085	64.5 ± 4.0	70.9 ± 4.0	5
N III* .	991.577 ^f	2.085 ^b	26.1 ± 2.3	7.8 ± 4.4	...
O I	950.884	0.176	13.4 ± 2.3	29.1 ± 5.6	6
	929.517	0.329	27.3 ± 3.0	...	7
	1026.476 ^g	0.434	4.3 ± 2.1	-0.01 ± 3.0	...
	976.448	0.509	7.5 ± 2.3	58.2 ± 6.0	...
	936.630	0.534	32.5 ± 2.4	40.6 ± 4.7	8
	948.685	0.778	50.4 ± 3.0	69.9 ± 6.9	9
	1039.230 ^h	0.980	67.5 ± 1.5	93.8 ± 1.8	10
	971.738	1.128	55.5 ± 3.6	124.0 ± 13.2	11
	988.773 ⁱ	1.737 ^b	162.5 ± 3.0	184.6 ± 7.5	12

Table 2—Continued

Species	λ (Å)	$\log(f\lambda)^a$	WD 2211 – 495 [$W_\lambda(\text{mÅ})$]	WD 2331 – 475 [$W_\lambda(\text{mÅ})$]	Ident. in Fig. 1
Ar I ^j ...	1048.218 ^k	2.440	15.1 ± 1.0	22.5 ± 1.8	13
Ar II ..	919.781	0.911	...	0.3 ± 6.1	...

^aFrom a privately distributed update by D. C. Morton to his compilation published earlier (Morton 1991).

^bTwo or more lines blended; line strength is for all of them combined.

^cThe large uncertainty is caused by an uncertain continuum in the vicinity of the closely spaced higher Lyman series transitions of H I.

^dIn principle, our upper limits for the column densities of N II in the excited fine structure levels, N II* and N II**, may be compared to lower limits for the amount of unexcited N II to arrive at a limit for the representative electron density (McKenna et al. 1996). Toward WD 2211 – 495 and WD 2331 – 475 we conclude that if $T = 7000\text{K}$, $n(e) < 0.8$ and 2.0cm^{-3} , respectively, but these values are higher than our actual expectations for the LISM based on C II*/C II and Mg I/Mg II seen elsewhere (Lallement & Ferlet 1997; Wood & Linsky 1997; Jenkins, Gry, & Dupin 2000).

^eG191-B2B: $51.0 \pm 4.1\text{mÅ}$; GD 394: $15.5 \pm 10.9\text{mÅ}$. This line could have interference from an absorption by Si II $\lambda 989.873$, but it is not likely to be strong.

^fG191-B2B: $-2.4 \pm 4.0\text{mÅ}$; GD 394: $15.4 \pm 10.0\text{mÅ}$.

^gG191-B2B: $1.3 \pm 2.7\text{mÅ}$; not measured for GD 394. This line consistently gave lower than expected absorption, based on the outcomes from other lines and the relative f -values. Hence, the published f -value for this line may be too large. For this reason, we disregarded indications from this line.

^hG191-B2B: $35.5 \pm 1.8\text{mÅ}$; GD 394: $51.9 \pm 3.4\text{mÅ}$.

ⁱG191-B2B: $88.4 \pm 3.9\text{mÅ}$; GD 394: $139.4 \pm 11.0\text{mÅ}$.

^jThe line of Ar I at 1066.66Å was not measured because of possible confusion with photospheric features of Si IV at 1066.61 , 1066.64 and 1066.65Å .

^kG191-B2B: $4.1 \pm 1.5\text{mÅ}$; GD 394: $12.0 \pm 2.9\text{mÅ}$.

3. Results

The first and second columns in Table 2 show the species and the wavelengths of their transitions that we measured within the broad spectral coverages for WD 2211 – 495 and WD 2331 – 475, with the lines ranked according to their strengths expressed in terms of $\log(f\lambda)$ (column 3) in each group. The fourth and fifth columns show the equivalent widths (in mÅ) and their errors arising from noise and uncertainties in the continuum and background levels. Our noise estimate was derived from the sizes of flux deviations from the adopted continuum level and thus included the effect of counting statistical fluctuations and small variations in the response of the detector (flat-field corrections were not made). Results for the more limited set of lines that we could measure for G191-B2B and GD 394 are given in the endnotes of the table.

White dwarf stars can have narrow, photospheric features that could interfere with or masquerade as interstellar lines. This problem is probably more severe for the stars GD 394 and WD 2211 – 495, which are known to be metal rich (Wolff et al. 1998). For example, the 952.3 Å feature of N I in WD 2211 – 495 is probably enhanced by a stellar feature, since the observed equivalent width is far higher than those of other transitions of comparable strength.

Table 3 summarizes our best estimates for the column densities of N I, O I, and Ar I, along with the values for $N(\text{H I})$ reported by other investigators. A velocity dispersion $b = 7 \text{ km s}^{-1}$ was derived for the O I lines toward WD 2211 – 495. The equivalent widths for the N I lines for this star are consistent with this b -value. Toward WD 2331 – 475 the N I lines give a best fit to $b = 6 \text{ km s}^{-1}$, while the O I lines are more consistent with $b = 10 \text{ km s}^{-1}$. This behavior probably arises from strong contrasts in physical environments for two or more velocity subcomponents, leading to different ratios of O I to N I in each case. For cases where the lines could not be seen or were marginally detected, we list upper limits for the column densities computed for the measurements plus their 2σ errors, assuming that the lines have no saturation. For such cases, a large wavelength interval ($\sim 0.3\text{Å}$) had to be considered (thus increasing the errors), because our wavelength scale was not very accurate.

Our ultimate objective was to judge the column densities in the light of a simple expectation based on some meaningful cosmic abundance scale. The entries within parentheses in Table 3 show how strongly deficient the neutral forms of these elements are with respect to their expected abundances relative to hydrogen, using the abundances in B stars as a standard.

Table 3. Neutral Atoms: Logarithms of Column Densities (cm^{-2}) and Deficiencies^a

Species	G191-B2B	GD 394	WD 2211 – 495	WD 2331 – 475
H I	18.36 ^b	18.65 ^{+0.16c} _{-0.34}	18.76 ^d	18.93 ^d
N I	13.90 ^b (−0.26)	13.85 ± 0.15 ^e (−0.60)	14.02 ± 0.15 (−0.54)	14.61 ± 0.15 (−0.12)
O I	14.84 ^b (−0.19)	14.94 ± 0.20 ^f (−0.38)	15.32 ^{+0.1} _{-0.3} (−0.11)	15.45 ± 0.1 (−0.15)
Ar I . . .	< 12.44 (< −0.42)	12.70 ± 0.1 (−0.45)	12.83 ± 0.1 (−0.43)	13.06 ± 0.1 ^g (−0.37)

^aValues in parentheses indicate by what logarithmic amount the abundances relative to H I deviate from their respective values in B stars, for which N = 7.80 (Cunha & Lambert 1994), O = 8.67 (Cunha & Lambert 1992) and Ar = 6.50 (Holmgren et al. 1990; Keenan et al. 1990) on a scale where H = 12.00.

^b (Vidal-Madjar et al. 1998).

^c (Barstow et al. 1996).

^d (Wolff et al. 1998); no errors stated.

^eFrom an observation of the N I multiplet at 1200 Å with GHRS on HST, reported by Barstow et al. (1996). While an arbitrarily large value of b gives a best fit to the lines, we expect that $b \approx 10 \text{ km s}^{-1}$ is more reasonable (and still gives an acceptable fit).

^fBased on our observations of the O I lines, but using $b = 10 \text{ km s}^{-1}$ (see note *e* above).

^g $b = 6 \text{ km s}^{-1}$ was adopted, as indicated by N I. The result drops to 13.01 if $b = 10 \text{ km s}^{-1}$ (from O I).

4. Interpretation

The deficiency of Ar I for all four stars is of order -0.4 dex. We adopt the argument presented by Sofia & Jenkins (1998) that this is not caused by Ar depleting onto the surfaces of dust grains, but rather that neutral Ar is more easily photoionized than H. If some photons with $E > 13.6$ eV can penetrate a region, the H can be partially ionized. Under these circumstances the Ar (I.P. = 15.76 eV) should be much more fully ionized because its photoionization cross section is about ten times that of H over a broad range of energies.

N I and O I also have photoionization cross sections that are larger than that of H I, but the ionization fractions of N and O are coupled to that of H via resonant charge exchange reactions. For O II, the rate coefficient for charge exchange with H I ($\sim 10^{-9}\text{cm}^3\text{s}^{-1}$) (Field & Steigman 1971) is much larger than the coefficient of recombination with free electrons ($4 \times 10^{-13}\text{cm}^3\text{s}^{-1}$ for $T = 7000\text{K}$), so the coupling of the O and H ionization fractions is very strong, unless there is appreciable ionization of O to higher stages. N II has a charge exchange rate that is only about twice the recombination coefficient (Butler & Dalgarno 1979), so in regions where $n_e \gg n_H$, N can start to behave more like Ar and show a deficiency of its neutral form.

To illustrate the expected deviations for O I/H I, N I/H I and Ar I/H I away from the condition where all three elements are fully neutral, Fig. 2 shows the results of our calculations of photoionization equilibria for various depths of shielding by neutral H and He within a cloud. The detailed equations and how they are solved are described by Sofia & Jenkins (1998). At any point within the cloud the radiation field caused by hot stars was assumed to be stronger or weaker than Vallergera’s (1998) combined stellar fluxes by a factor $\exp\{[9 \times 10^{17}\text{cm}^{-2} - N(\text{H I})][\sigma(\lambda)_{\text{H I}} + 0.07\sigma(\lambda)_{\text{He I}}]\}$, where the $\sigma(\lambda)$ ’s are the photoionization cross sections. We supplemented this field with Slavin’s (1989) calculated flux from a cloud’s conductive interface with much hotter gases.¹¹

Turning back to the observations, the results shown in Table 3 indicate that N and O are deficient, but for G191-B2B and WD 2331 – 475 not as strongly as Ar. A mild deficiency in N can be understood if the hydrogen is mostly ionized, as is expected near the boundary of a cloud (see Fig. 2). The importance of ionization in reducing N I is reinforced by our lower limits (assuming no saturations of the profiles) for $[\log N(\text{N II}), \log N(\text{N III})] = [\text{unavail.}, 13.68], [13.86, 13.78], [13.68, 13.82]$ toward G191-B2B, WD 2211 – 495 and WD 2331 – 475. Here, we can state that *at least* 38, 56 and 22% of all the nitrogen is in an

¹¹We attenuated the strong emission peak near 70 \AA caused by Fe IX, Fe X and Fe XI, recognizing that McCammon et al. (2000) failed to observe these lines at a flux level far below the predicted one. This probably happens because Fe is depleted onto dust grains.

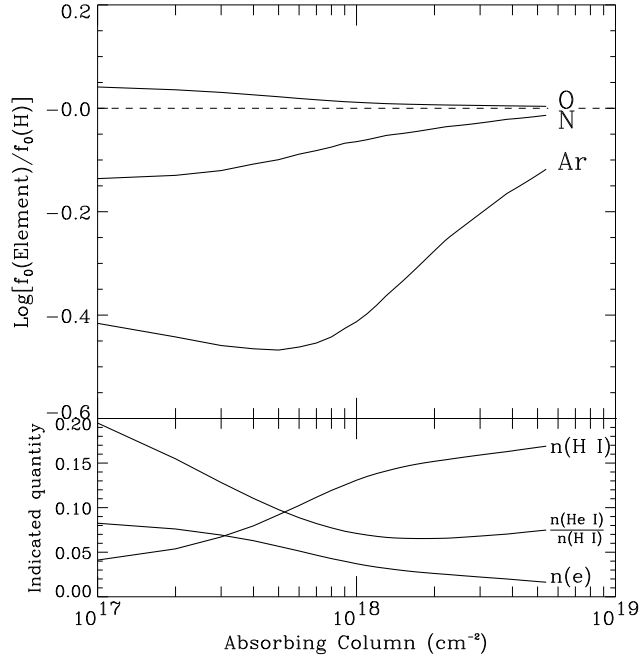


Fig. 2.— Top panel: Logarithms of the expected deficiencies of the neutral fractions $f_0 = n(\text{neutral})/n(\text{total})$ of N, O and Ar, compared to those of H, caused by photoionization arising from the radiation by hot stars and a hot-gas conduction front surrounding a LISM cloud. These fractions are plotted as a function of the shielding depths [scaled to $N(\text{H I})$] within a cloud at a uniform pressure $p/k = 1.5 \times 10^3 \text{cm}^{-3}\text{K}$ and temperature $T = 7000\text{K}$. Local densities of neutral hydrogen and electrons (in cm^{-3}) and the ratio of neutral H to He are shown in the bottom panel.

ionized form toward the respective stars. The underabundances of O are harder to explain, although they are reduced in magnitude by 0.17 dex if one adopts as a standard the O/H found in the ISM by Meyer, et al. (1998) (8.50 on a logarithmic scale with $H = 12.00$) rather than the value of O/H in B stars. Also, in view of the possibly large uncertainties in $N(\text{H I})$ (except for G191-B2B), it may be better to adopt O as the reference element instead of H when we investigate the behavior of N I and Ar I.

For GD 394 and WD 2211 – 495, it is difficult to understand why the deficiencies of N I are not much weaker than the corresponding ones of Ar I. One possible explanation could be that a conduction front is not the dominant source of high energy radiation, but instead the ionization of N and Ar might be strongly influenced by 40 – 80 eV photons arising from recombinations to He II, which could conceivably be the dominant form of diffuse EUV radiation (Breitschwerdt, 2000) if much of the material in the Local Bubble has cooled to $T \lesssim 10^5 \text{K}$ but has not yet recombined (Breitschwerdt & Schmutzler 1994). Over much of this energy range, N I is more easily ionized than Ar I if recombinations with free electrons are more important than charge exchange with H I [see Fig. 3 of Sofia & Jenkins (1998)]. It will be interesting to see if detailed calculations confirm this conjecture.

A flux of ionizing photons with $E > 24.6 \text{ eV}$ and sufficient intensity to create the steady-state ionization of He in the LISM has not yet been observed directly, but our observations showing a significant reduction in Ar I favor its existence. If, by contrast, we had found a normal amount of Ar I, we might have concluded that the gas was probably more highly ionized in the past and has not yet fully recombined. Here, a near equality of Ar I/H I to the expected cosmic ratio would have arisen from their virtually identical recombination coefficients. Ionizations to levels higher than the singly ionized forms are not important in this picture, since their recombination rates are significantly faster ($\propto Z^2$).

We thank T. M. Tripp and C. Howk for their review and comments on an early draft of this paper.

REFERENCES

- Barstow, M. A., Holberg, J. B., Hubeny, I., Lanz, T., Bruhweiler, F. C., & Tweedy, R. W. 1996, *MNRAS*, 279, 1120
- Breitschwerdt, D. 2000, private communication
- Breitschwerdt, D., & Schmutzler, T. 1994, *Nat*, 371, 774
- Butler, S. E., & Dalgarno, A. 1979, *ApJ*, 234, 765

- Cox, D. P., & Reynolds, R. J. 1987, *ARA&A*, 25, 303
- Cunha, K., & Lambert, D. L. 1992, *ApJ*, 399, 586
- 1994, *ApJ*, 426, 170
- Dupuis, J., Vennes, S., Bowyer, S., Pradhan, A. K., & Thejll, P. 1995, *ApJ*, 455, 574
- Ferlet, R. 1999, *A&A Rev.*, 9, 153
- Field, G. B., & Steigman, G. 1971, *ApJ*, 166, 59
- Frisch, P. C., & Slavin, J. D. 1996, *Space Sci. Rev.*, 78, 223
- Gry, C. 1996, *Space Sci. Rev.*, 78, 239
- Holmgren, D. E., Brown, P. J. F., Dufton, P. L., & Keenan, F. P. 1990, *ApJ*, 364, 657
- Jenkins, E. B., Gry, C., & Dupin, O. 2000, *A&A*, 354, 253
- Keenan, F. P., Bates, B., Dufton, P. L., Holmgren, D. E., & Gilheany, S. 1990, *ApJ*, 348, 322
- Lallement, R. 1996, *Space Sci. Rev.*, 78, 361
- Lallement, R., & Ferlet, R. 1997, *A&A*, 324, 1105
- Lallement, R., Linsky, J. L., Lequeux, J., & Branov, V. B. 1996, *Space Sci. Rev.*, 78, 299
- Linsky, J. L. 1996, *Space Sci. Rev.*, 78, 157
- Lyu, C. H., & Bruhweiler, F. C. 1996, *ApJ*, 459, 216
- McCammon, D., Almy, R., Apodaca, E., Bergmann, W., Deiker, S., Galeazzi, M., Lesser, A., Sanders, W., Figueroa, E., Kelley, R. L., Porter, F. S., Stahle, C. K., & Szymkowiak, A. E. 2000, *BAAS*, in press (late paper nr. 135.04, AAS Atlanta meeting)
- McKenna, F. C., Keenan, F. P., Foster, V. J., Jenkins, E. B., Bell, K. L., & Stafford, R. P. 1996, in *UV and X-ray Spectroscopy of Astrophysical and Laboratory Plasmas*, ed. K. Yamashita & T. Watanabe (Tokyo: Universal Academy Press), p. 499
- Meyer, D. M., Jura, M., & Cardelli, J. A. 1998, *ApJ*, 493, 222
- Moos, H. W. et al. 2000, *ApJ*, this issue
- Morton, D. C. 1991, *ApJS*, 77, 119
- Redfield, S., & Linsky, J. L. 2000, *ApJ*, submitted
- Reynolds, R. J. 1986, *AJ*, 92, 653
- Sahnou, D. J. et al. 2000, *ApJ*, this issue
- Sfeir, D. M., Lallement, R., Crifo, F., & Welsh, B. Y. 1999, *A&A*, 346, 785

- Slavin, J. D. 1989, *ApJ*, 346, 718
- Slavin, J. D., & Frisch, P. C. 1998, in *The Local Bubble and Beyond*, ed. D. Breitschwerdt, M. J. Freyberg, & J. Trümper (Berlin: Springer), p. 305
- Sofia, U. J., & Jenkins, E. B. 1998, *ApJ*, 499, 951
- Vallerga, J. 1998, *ApJ*, 497, 921
- Vidal-Madjar, A., Lemoine, M., Ferlet, R., Hébrard, G., Koester, D., Audouze, J., Cassé, M., Vangioni-Flam, E., & Webb, J. 1998, *A&A*, 338, 694
- Wolff, B., Koester, D., Dreizler, S., & Haas, S. 1998, *A&A*, 329, 1045
- Wolff, B., Koester, D., & Lallement, R. 1999, *A&A*, 346, 969
- Wood, B. E., & Linsky, J. L. 1997, *ApJ*, 474, L39